Modelling Thermal Radiation Effects on Temperature and Concentration on Magnetohydrodynamic Flow in the Presence of Chemical Reaction in a Porous Medium

[1*]Lawal A. O. Jimoh O.R. and Yusuf S. I.

[1]Department of Mathematics, Federal University of Technology, Minna, Nigeria

Phone : +2348167823987,+2348077808699, +2347069297464

[1*]Corresponding author: [1]azeez.lawal@st.futminna.edu.ng,

Abstract

This study presents a mathematical model that explores the impact of thermal radiation effects on temperature and concentration on magnetohydrodynamic (MHD) flow in the presence of chemical reaction in a porous medium. The governing partial differential equations were non-dimensionalized, transformed to ordinary differential equations using harmonic solution technique and solved using perturbation method. The results which were presented graphically, highlight several key observations. Specifically, an increase in Grashof number, Dufour number, and porosity parameter leads to higher velocity profiles. Furthermore, Radiative parameters are found to reduce the fluid temperature. The findings of this work will be crucial in optimizing processes in areas like combustion, cooling systems and environmental control technology where such complex interactions are prevalent.

Keywords: Dufour number, Grashof number, harmonic solution technique, Magneto-hydrodynamic

1.**Introduction**

In many scientific, industrial, and environmental applications, natural convection arising from the buoyancy effect produced by density changes in a fluid is one of the key phenomena affecting such cases. Such applications include nuclear waste disposal, catalytic reactors, and energy systems requiring efficient temperature control and security (Riley et al., 2006). Jimoh and Abdullahi (2023) examined the effect of chemical reaction and viscous dissipation in MHD flow over an inclined porous plate for heat and mass transfer. They discovered that an increase in Peclet number, Grashof number, and heat source parameter strengthens velocity and temperature profiles. The internal energy dissipation modified the thermal and concentration boundary layers.

Zubi (2018) examined the conducting fluid and material flow of an to and fro movement flow over a perpendicular Porous medium. He discovered that the fluid velocity rises when the parameters of the interaction species and porous rises, and also rises when the parameters of magnetism reduce.Sandhya *et al*. (2020) investigated how Magnetohydrodynamics flow across a perpendicular flow passage during a chemical reaction is affected by mass and heat transfer. The thermal diffusion influence an perpendicular plate on the flow region have been attempted to be explained with the aid of the thermal region, interaction species,and heat emission. To solve the dimensional higher derivatives equations, the closed analytical approach was applied. As the Grashof, modified Grashof, and Soret numbers increase, the fluid velocity also increases

3. Model Formulation

In this study, the effects of a variable temperature and concentration inclined moving plate under an external transverse field and flowing through porous medium the unsteady free convection viscous incompressible radiative fluid were investigated. A Cartesian coordinate system is set up, where the x-axis is taken along the plate while the y-axis is taken normal to it. A field of strength B, would act on the system perpendicularly to the plate in the y-direction such that it influences the motion of the electrically conducting fluid. The plate has been inclined with respect to the horizontal by an angle θ, which provides a more realistic representation of practical applications such as geophysical fluid dynamics, industrial heat exchangers, and astrophysical flows. Low magnetic Reynolds numbers give rise to a consideration of induced field being negligible, such that it is the applied field only which acts on the flow.

It is assumed initially that both the fluid and plate are kept at equal temperature $T0$ and concentration $C0$ thereby establishing a thermodynamic equilibrium. For time t>0, the plate is supposed to be accelerated exponentially with a velocity function U(t)in its own plane. At the same time temperature and concentration at the plate surface are assumed to vary linearly with time giving an unsteady thermal and solutal boundary condition. This study also considers a strong chemical reaction that takes part in the fluid species, which affects the concentration profiles as well as diffusion rates. The radiative heat transfer is assumed to consider that the fluid is optically thin gray medium in which no scattering takes place, thus only emission and absorption contributes for the exchange of radiative energy. This gives a special formulation to capture how the combined effects of magnetism, radiation, chemical reaction and porous media would affect temperature, concentration and velocity distribution in an MHD flow system and provides useful insight into engineering and environmental applications.

$$\frac{\partial u^*}{\partial t^*} = g\beta(T^* - T^*{}_\infty)\cos\gamma + g\beta^*(\mathrm{C}^* - C_\infty{}^*)\cos\gamma + \frac{v\partial^2 u^*}{\partial y^{*2}} - \frac{\sigma B_o{}^2 u^*}{\rho} - \frac{vu^*}{k_p{}^*} \tag{1}$$

$$\rho c_p \frac{\partial T^*}{\partial t^*} = k\frac{\partial^2 T}{\partial y^{*^2}} - 16a^* T^{*^3}{}_\infty (T^* - T_\infty{}^*) + S^*(T^* - T_\infty{}^*) + \frac{D_m k_T}{c_s c_p}\frac{\partial^2 c^*}{\partial y^{*^2}} \tag{2}$$

$$\frac{\partial C^*}{\partial t^*} = D_m \frac{\partial^2 c^*}{\partial y^{*^2}} - K_c{}^*(\mathrm{C}^* - C_\infty{}^*) \tag{3}$$

Where,

u^* is the velocity on horizontal component

a^* absorption coefficient

ν static internal friction

u_o is the velocity on fluid,

g constant gravity of the earth,
a is the accelerating parameter,

β is a measure of how much a material's volume increases in response to a change in temperature.,

β^* refers to the measure of how the volume of a substance changes in response to variations in mass transfer processes, particularly when influenced by temperature changes.,

K_p^* is a measure of the medium's ability to allow fluids, such as liquids or gases, to flow through its interconnected pore spaces.,

q_r refers to the rate at which thermal energy is transferred through electromagnetic radiation across a given surface area.,
∞ is incline angle
σ is the heat conducting fluid ,
T^* degree flow

T_∞^* distance degree flow,

K amount of heat energy flow
K_c^* reaction species,
S^* heat source parameter,

c_p heat at constant pressure,

C^* amount of solute presence,

C^*_∞ distance solute presence,

D_r is the Dufour number
D_m is the mass diffusivity,
The initial and boundary conditions are given by,

$$\left.\begin{array}{l} u^*(y^*,0)=0, \quad u^*(0,\mathrm{t})=u_o e^{a^*t^*}, \quad u^*(y^*\to\infty,t)\to 0 \\ T^*(y^*,0)=T_\infty{}^*, \quad T^*(0,\mathrm{t})=T_\infty{}^*+\left(\dfrac{T_w{}^*-T_\infty{}^*}{v}\right)u_o{}^2t^* \quad T^*(y^*\to\infty,t)\to \mathrm{T}_\infty{}^* \\ C^*(y^*,0)=C_\infty{}^* \quad C^*(0,t)=C_\infty{}^*+\left(\dfrac{C_w{}^*-C_\infty{}^*}{v}\right)u_o{}^2t^* \quad C^*(y^*\to\infty,t)\to C_\infty{}^* \end{array}\right\} \tag{4}$$

Non – dimensionalisation

Equations (1), (2), (3), and (4) are non-dimensionalised using the following dimensionless variables

$$y=\frac{y^*u_o}{v}, \quad t=\frac{u_o{}^2t^*}{v}, \quad , \quad \theta=\frac{T^*-T_\infty{}^*}{T_w{}^*-T_\infty{}^*} \quad \phi=\frac{C^*-C_\infty{}^*}{C_w{}^*-C_\infty{}^*}, \qquad u=\frac{u^*}{u_o} \tag{5}$$

After non-dimensionalization, equations (1), (2), (3) and (4) becomes

$$\frac{\partial u}{\partial t}=G_{r\theta}\theta\cos\gamma+G_{m\phi}\phi\cos\gamma+\frac{\partial^2 u}{\partial y^2}-Mu-\frac{u}{K_p} \tag{6}$$

$$\frac{\partial\theta}{\partial t}=\frac{1}{P_r}\frac{\partial^2\theta}{\partial y^2}-\frac{R}{P_r}\theta+S\theta+D_r\frac{\partial^2\phi}{\partial y^2} \tag{7}$$

$$\frac{\partial\phi}{\partial t}=\frac{1}{S_c}\frac{\partial^2\phi}{\partial y^2}-K_c\phi \tag{8}$$

$$\left.\begin{array}{lll} u(\mathrm{y},0)=0, & u(0,t)=e^{at}, & u(\mathrm{y}\to\infty,\mathrm{t})=0 \\ \theta(y,0)=0, & \theta(0,\mathrm{t})=\mathrm{t}, & \theta(y\to\infty,t)=0 \\ \phi(y,0)=0, & \phi(0,t)=t, & \phi(y\to\infty,t)=0 \end{array}\right\} \tag{9}$$

Where,

$$\left.\begin{array}{l} M=\dfrac{\sigma\beta_o{}^2v}{\rho u_o{}^2}, \quad K_c=\dfrac{vK_c{}^*}{u_o{}^2}, \quad G_{r\theta}=\dfrac{g\beta v\left(T^*-T_\infty{}^*\right)}{u_o{}^3} \quad G_{r\phi}=\dfrac{g\beta v\left(C^*-C_\infty{}^*\right)}{u_o{}^3} \\ S_c=\dfrac{v}{D} \quad R=\dfrac{16a^*v^2\sigma T^*{}_\infty}{ku_o{}^2} \quad S=\dfrac{S^*v}{\rho C_p u_o{}^2} \quad K_p=\dfrac{u_o{}^2K_p{}^*}{v^2} \\ P_r=\dfrac{\mu C_p}{K} \quad R=\dfrac{16a^*\sigma^*v^2T_\infty{}^{*3}}{Ku_o{}^2} \quad D_r=\dfrac{D_m k_T\left(C_w{}^*-C_\infty{}^*\right)}{vC_sC_p\left(T_w{}^*-T_\infty{}^*\right)} \end{array}\right\} \tag{10}$$

Materials and Methods

The aforementioned equations (6), (7) and (8) are the interconnected partial differential equations that give an efficient approach to solving them by using harmonic solution method. This method helps in the transformation of PDEs to a system of ordinary differential equations with subsequent analytical solution. The analytical solution will then take the form in which the fluid velocities, temperatures, and concentrations in the area close to the plate are expressed as follows:

$$u(y,t)=u(y)e^{iwt},\ \theta(y,t)=\theta(y)e^{2iwt},\ \phi(y,t)=\phi(y)e^{iwt}, \tag{11}$$

By Substituting equation (11) into equations (6), (7), and (8), the following equations are obtained:

$$\frac{d^2u}{dy^2} - c_1^2 = -G_{r\theta}e^{i\omega t}\theta\cos\gamma - G_{r\phi}\phi\cos\gamma \tag{12}$$

$$\frac{d^2\theta}{dy^2} - c_2^2\theta = -D_rP_re^{-iwt}\frac{d^2\phi}{dy^2} \tag{13}$$

$$\frac{d^2\phi}{dy^2} - c_3^2\phi = 0 \tag{14}$$

Let

Let $c_1 = \sqrt{\left(iw + M + \frac{1}{K_p}\right)}$ (15)

$$c_2 = \sqrt{\left(\frac{R}{P_r} - S + 2iw\right)P_r} \tag{16}$$

$$C_3 = \sqrt{(iw + K_c)S_c} \tag{17}$$

Equations (6), (7), and (8) becomes

$$\left.\begin{aligned} &\frac{d^2u}{dy^2} - c_1^2 = -G_{r\theta}e^{iwt}\theta\cos\gamma - G_{r\theta}\phi\cos\gamma \\ &u(0) = \frac{e^{at}}{e^{iwt}} \quad u(y\to\infty) = 0 \end{aligned}\right\} \tag{18}$$

$$\left.\begin{aligned} &\frac{d^2\theta}{dy^2} - c_2^2\theta = -D_rP_re^{-iwt}\frac{d^2\phi}{dy^2} \\ &\theta(0) = \frac{t}{e^{2iwt}},\ \theta(y\to\infty) = 0 \end{aligned}\right\} \tag{19}$$

$$\left.\begin{aligned}&\frac{d^2\phi}{dy^2}-c_3{}^2\phi=0\\&\phi(0)=\frac{t}{e^{iwt}},\phi(y\to\infty)=0\end{aligned}\right\}$$

By applying perturbation method, Let

$$\left.\begin{aligned}u&=u_o+G_{r\theta}u_1+G^2{}_{r\theta}u_2+...\\\theta&=\theta_o+G_{r\theta}\theta_1+G^2{}_{r\theta}\theta_2+...\\\phi&=\phi_o+G_{r\theta}\phi_1+G^2{}_{r\theta}\phi_2+...\end{aligned}\right\}\quad(20)$$

By substituting equations (21) into (18), (19) and (20) and equating corresponding terms on both sides, the following equations are obtained:

For order 0, $G_{r\theta}{}^0:1$,

$$\left.\begin{aligned}&\frac{d^2u_o}{dy^2}-c_1{}^2u_o=0\\&u_o(0)=\frac{e^{at}}{e^{iwt}},\quad u_o(y\to\infty)=0\end{aligned}\right\}\quad(21)$$

$$\left.\begin{aligned}&\frac{d^2\theta_o}{dy^2}-c_2{}^2\theta_o=-D_rP_re^{-iwt}\frac{d^2\phi_o}{dy^2}\\&\theta_o(0)=\mathrm{te}^{-2iwt},\quad \theta_o(y\to\infty)=0\end{aligned}\right\}\quad(22)$$

$$\left.\begin{aligned}&\frac{d^2\theta_o}{dy^2}-c_2{}^2\theta_o=-D_rP_re^{-iwt}\frac{d^2\phi_o}{dy^2}\\&\phi_o(0)=te^{-iwt}\quad \phi_o(y\to\infty)=0\end{aligned}\right\}\quad(23)$$

For order 1, $G_{r\theta}{}^1,:G_{r\theta}$

$$\left.\begin{aligned}&\frac{d^2u_1}{dy^2}-c_1{}^2u_1=-e^{iwt}\cos\phi\theta_o-\cos\gamma\phi_o\\&u_1(0)=0,\quad u_1(y\to\infty)=0,\end{aligned}\right\}\quad(24)$$

$$\left.\begin{aligned}&\frac{d^2\theta_1}{dy^2}-c_2{}^2\theta_1=-D_rP_re^{-iwt}\frac{d^2\phi_1}{dy^2}\\&\theta_1(0)=0,\quad \theta_1(y\to\infty)=0,\end{aligned}\right\}\quad(25)$$

$$\left.\begin{aligned} &\frac{d^2\phi_1}{dy^2} - c_3{}^2\phi_1 = 0 \\ &\phi_1(0) = 0, \quad \phi_1(y \to \infty) = 0 \end{aligned}\right\} \tag{26}$$

The boundary value problems (22) to (27) are solved by the method of undetermined coefficients and obtained the following results:

$$u(y) = A_2 e^{-c_1 y} + G_{r\theta}\left(A_9 e^{-c_1 y} + A_{10} e^{-c_2 y} + A_{11} e^{-c_3 y}\right) \tag{28}$$

$$\theta(y) = A_6 e^{-c_2 y} + A_7 e^{-c_3 y} + G_{r\theta}\left(A_{15} e^{c_2 y} + A_{16} e^{-c_3 y}\right) \tag{29}$$

$$\phi(y) = A_4 e^{-c_3 y} + G_{r\theta}\left(A_{13} e^{-c_3 y}\right) \tag{30}$$

The general solution of equations (1), (2) and (3) with the associated boundary and initial conditions (4) is therefore in the form of:

$$\left. u(y,t) = u(y)e^{iwt} \quad \theta(y,t) = \theta(y)\,\mathrm{e}^{2iwt} \quad \phi(y,t) = \phi e^{iwt} \right\} \tag{31}$$

RESULTS

This part elaborates on the effects of important dimensionless parameters on fluid velocity, temperature distribution, and concentration of species. The Grashof number, thermal interaction species variable, radiation parameter, Schmidt number, Dufour number, porosity parameter, and field parameter were some of the considered parameters.

3.1 Figures

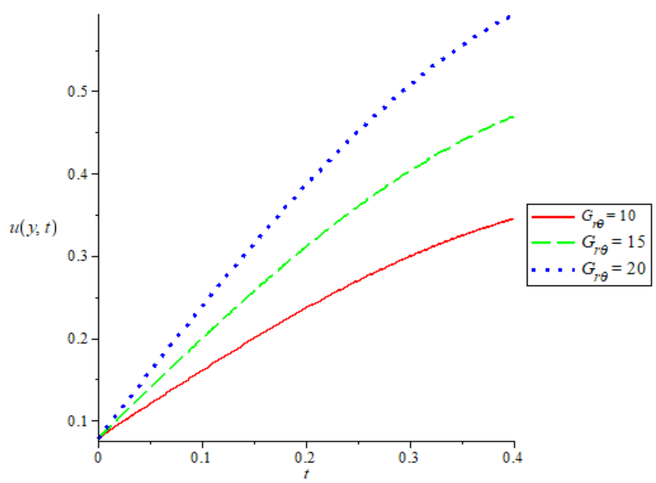

Figure 1 : Graph of Velocity $u(y,t)$ against Time (t) for varies Values of thermal Grashof number $(G_{r\theta})$.

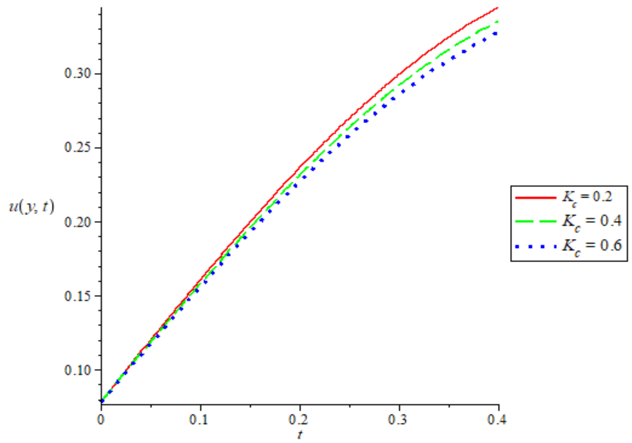

Figure 2 : Diagram of Velocity of the Fluid $u(y,t)$ against time (t) for varies Values of thermal Chemical reaction parameter (K_c).

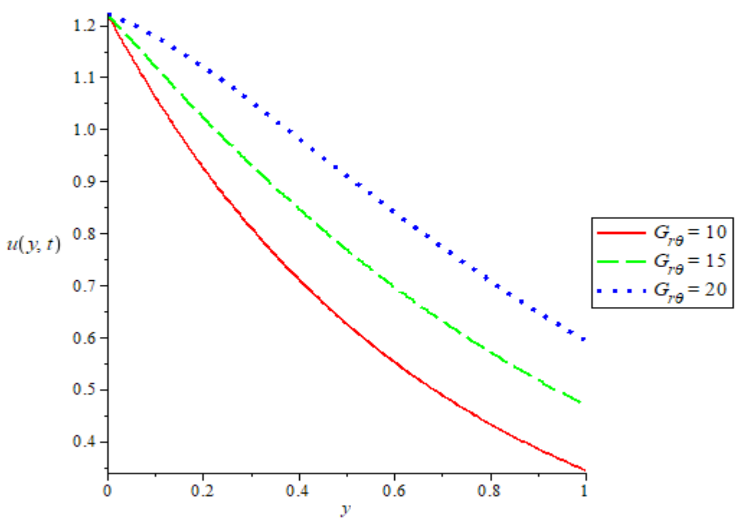

Figure 3 : Graph of Velocity of the Fluid $u(y,t)$ against Distance (y) for Different Values of thermal Grashof Number $(G_{r\theta})$.

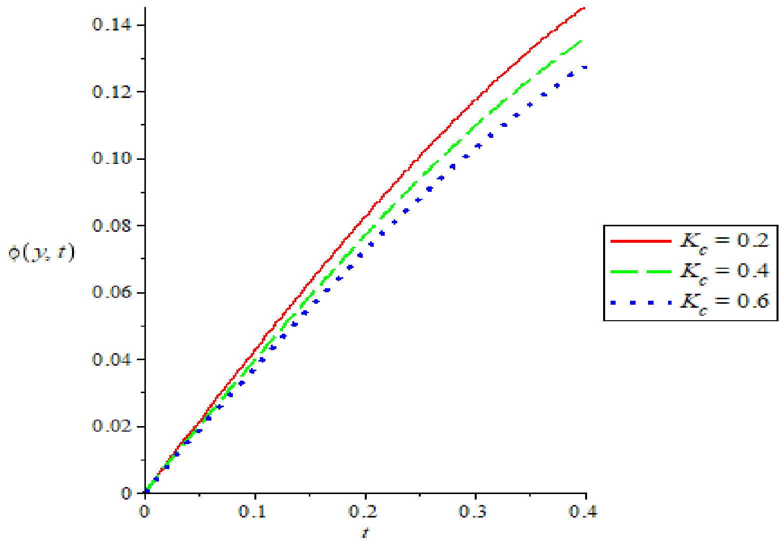

Figure 4 : Graph of Species Concentration $\phi(y,t)$ over **Time** (t) **for Different Values of thermal Chemical reaction parameter** (K_c)**.**

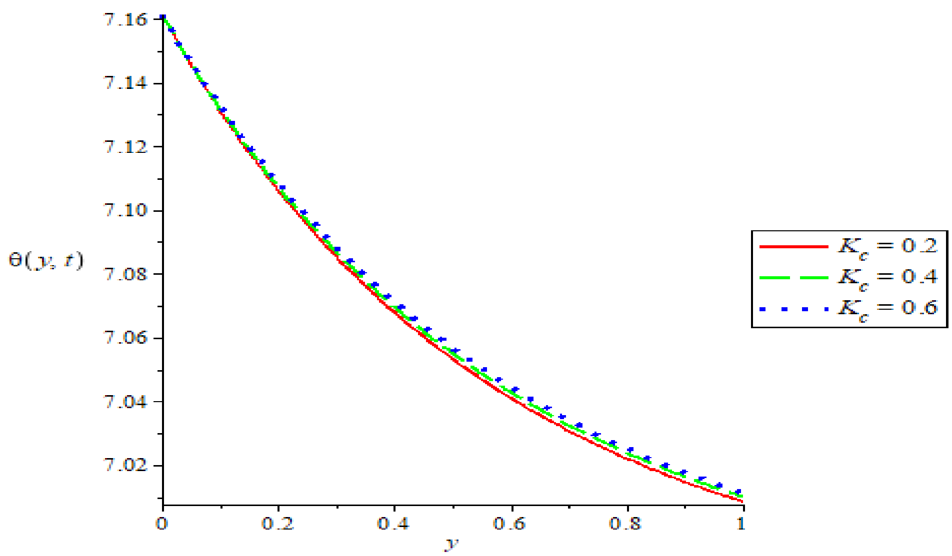

Figure 5 : Graph of Temperature of the Fluid $\theta(y,t)$ **against Distance** (y) **for Different Values of thermal chemical reaction parameter** (K_c)**.**

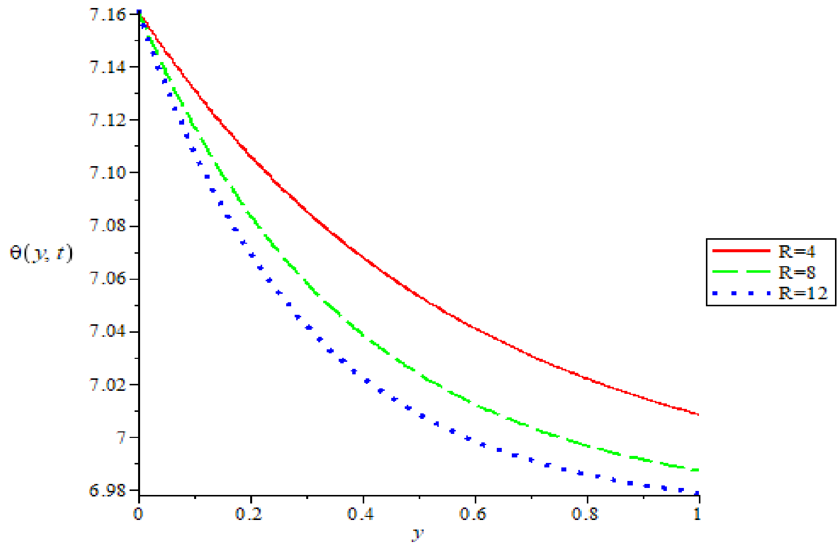

Figure 6 : Graph of Temperature $\theta(y,t)$ against Distance (y) for Different Values of Radiative variables (R).

4. Results and Discussion

Figure 1 shows how the fluid's flow changes on time in relation to thermal Grashof number. It is observed that the velocity of the fluid $u(y,t)$ rises faster with rise in the thermal Grashof number $(G_{r\theta})$ at steady time. Figure 2 show how the fluid's flow changes on time in relation to the thermal chemical reaction parameter. It is observed that the velocity of the fluid $u(y,t)$ reduces with rise in the thermal chemical reaction parameter (K_c).

Figure 3 shows how the heat Grashof Number affects the fluid's velocity as a function of distance. It is observed that the velocity of the fluid $u(y,t)$ rises faster with rise in the thermal Grashof number $(G_{r\theta})$ at steady time. Figure 4 shows the effect of thermal chemical reaction parameter on the concentration of the fluid .It is observed that the species concentration of the fluid $\phi(y,t)$ reduces with rise in the thermal Grashof number $(G_{r\theta})$ at steady time.

Figure 5 shows the effect of thermal chemical reaction parameter (K_c) on the temperature of the fluid $\theta(y,t)$.It is observed that temperature of the fluid $\theta(y,t)$ rises with rise in the thermal chemical reaction parameter (K_c) at steady time. Figure 6 shows the effect of the radiative parameter (R) on the temperature of the fluid $\theta(y,t)$.It is observed that the temperature of the fluid $\theta(y,t)$ reduces with rise in the thermal chemical reaction parameter (K_c) at steady time.

5. Conclusion

The analysis of mathematical model was studied out to examine how thermal radiation affects the degree of hotness and interaction species profiles in a Magnetohydrodynamic (MHD) flow within a porous material. The harmonic solution method was used to analytically solve the system's coupled, non-linear, dimensionless partial differential equations. Understanding the impact of different dimensionless parameters—which were graphically depicted on the behavior of the system was the main goal of the study. The results of this analysis shed important light on how various parameters affect the temperature distribution, species concentration, and fluid flow over time and space. With possible applications in domains like engineering, environmental science, and industrial processes where such conditions are pertinent, these findings advance our knowledge of heat and mass transport events in MHD flows under the impact of thermal radiation and chemical reactions.

In contrast, components like the Thermal Chemical Reaction, and Grashof number tend to decrease the fluid velocity over time, slowing down the flow; additionally, the Radiative Parameter was found to decrease the fluid's temperature against time, indicating its cooling effect; and finally, the Thermal Chemical Reaction and Schmidt number were observed to lower the species concentration against time, reflecting their impact on the distribution of species concentration in the fluid.

References

Jimoh, O.R. & Abdullahi, D. (2023): Effect of Heat and Mass Transfer on Magneto-Hydrodynamic Flow with Chemical Reaction and viscous energy dissipation past an inclined porous plate**.** *Scientia Africana, Vol. 22 (No. 2), Pp 259-276*

Riley, K. F., Hobson, M. P. & Bence, S. J. (2006). *Mathematical Methods for Physics and Engineers. Third Edition, Cambridge University Press, New York.*

Siti, K.S., Anuar, I.& Loan, P. (2017): Unsteady MHD flow and heat transfer over a shrinking sheet with Ohmic heating. *Chinese journal of physics* Vol. 55, pp 1626-1636.

Zubi, M.A. (2018): MHD heat and mass transfer of an oscillatory flow over a vertical permeable plate in a porous medium with chemical reaction. *Modern Mechanical Engineering 8 (3), 179-191*